Impedance Matching Characteristic Research Utilizing L-type Matching Network

Jun Gyu Ha[*,**], Bo Keun Kim[**,****] and Dae Sik Junn[***†]**

[*]Department of Electronics Engineering, Myongji University,
[**]Department of Electrical Engineering, Myongji University,
[***†]Department of Semiconductor Engineering, Myongji University,
[****]Semiconductor Equipment Engineering Program

ABSTRACT

If an impedance mismatch occurs between the source and load in a Radio Frequency transmission system, reflected power is generated. This results in incomplete power transmission and the generation of Reflected Power, which returns to the Radio Frequency generator. To minimize this Reflected Power, Impedance matching is performed. Fast and efficient Impedance matching, along with converging reflected power towards zero, is advantageous for achieving desired plasma characteristics in semiconductor processes. This paper explores Impedance matching by adjusting the Vacuum Variable Capacitor of an L-type Matching Module based on the trends observed in the voltage of the Phase Sensor and Electromotive Force voltage. After assessing the impedance matching characteristics, the findings are described.

Key Words : L-type Matching Network, Phase Sensor, Vacuum Variable Capacitor, Impedance Matching

1. Introduction

As semiconductor miniaturization progresses, it is a fundamental requirement to achieve consistent process results across different equipment or within the same equipment. In particular, in the etching process, ensuring uniform control over the Critical Dimension (CD) is one of the most critical aspects in semiconductor production. To achieve this, extensive research is being conducted, especially in the case of semiconductor equipment that utilizes plasma. Maintaining consistent plasma characteristics has become increasingly important, and as a result, significant research efforts are dedicated to this area. Therefore, in order to maintain consistent plasma characteristics, RF power is applied to the process chamber without any loss, utilizing impedance matching which minimizes differences between equipment.

Plasma sources can be categorized into two types: Capacitively Coupled Plasma (CCP) and Inductively Coupled Plasma (ICP). Both types, CCP and ICP, utilize RF (Radio Frequency) power to supply energy and create plasma within the chamber. In the semiconductor manufacturing process, when power is delivered to the chamber, the impedance inside the chamber changes as the process is carried out by the plasma. Consequently, RF reflected power occurs due to this impedance variation. This refers to the impedance mismatching between the source impedance and load impedance, resulting in the loss of RF power delivered from the source to the chamber. To minimize such reflected power, impedance matching is performed. By controlling it to converge to zero, it can contribute to maintaining plasma characteristics and reducing differences between equipment.

In response to this need, there are ongoing developments in South Korea for the automation of plasma impedance matching systems. Indeed, for reliable operation, there are active developments in the areas of high-reliability RF po-

[†]E-mail: davidjunn@mju.ac.kr

wer supplies, removal of high harmonic components to accommodate automated matching, efficient power amplifier design, and the development of automatic matching detectors and control technologies [3].

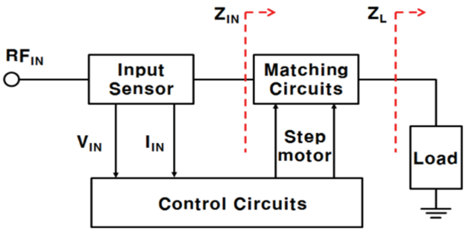

Fig. 1. Schematic of RF Delivery system. [2].

This paper focuses on the detection of RF signals through a phase sensor and the control of a step motor by the control unit (MCU) to achieve L-type impedance matching through VVC control. To achieve this, we designed the impedance matching algorithm and utilized the counter matcher to arbitrarily change the impedance. We then proceeded with impedance matching through the VVC control algorithm. After achieving impedance matching, we analyzed the characteristics of reflect power, phase sensor voltage, and capacitance (load, tune) to assess the performance.

2. Experimental

Fig. 2 depicts the configuration of the Phase Sensor in a visually understandable manner. According to the Fig. 2, there is an inner conductor inside the Coaxial line, surrounded by a Voltage Probe and a Current Probe for voltage and current detection, respectively. The Voltage Probe detects the voltage component by measuring the potential difference between the ground and the point where the electric field is applied to the inner conductor of the Coaxial line. The Current Probe is constructed with a coil wound in a perpendicular direction to the magnetic field flux around the inner conductor of the Coaxial line. This is because when a current flows through the inner Conductor of the Coaxial line, it generates a magnetic field. This magnetic field induces an electromotive force (EMF) voltage in the coil. The current component is obtained through the EMF voltage. The E-Field Shield serves to block electric field coupling that can cause errors in the current detector [2].

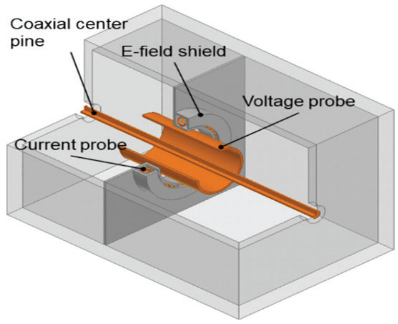

Fig. 2. Structure of Phase sensor. [2].

The RF Delivery System is a system designed to deliver RF power from the source to the load efficiently. Referring to Figure 1, we can observe the components involved in generating plasma, including the RF Power Supply (RF Generator), the INPUT Sensor (Phase Sensor) responsible for detecting the RF signal from the RF Power Supply, and the Matching Circuit (RF Matcher) used for impedance matching. When power reaches the chamber, the impedance inside the chamber changes due to the presence of plasma. To minimize Reflect Power and achieve maxi-mum power transfer without significant losses, impedance matching is performed in the RF Matcher. This involves adjusting the Load Impedance to match the Source Impedance, ensuring impedance compatibility between the RF power supply and the chamber. When RF power is applied and the process starts, the Phase Sensor sends phase and magnitude signals to the MCU. Based on these signals, the impedance matching algorithm is executed, which controls the motor driver to adjust the capacitance of the Variable Voltage Capacitor (VVC) connected to the Step Motor. This process allows for impedance matching, aligning the Load Impedance with the Source Impedance to minimize Reflect Power and optimize power transfer. The RF Generator has an internal impedance fixed at 50Ω. There-fore, theoretically, if the load impedance matches 50Ω, maximum power can be delivered.

$$
\begin{aligned}
P_{ave} &= \frac{1}{2} Re[V(z)I(z)*] \\
&= \frac{1}{2} Re\left[|V_0^+|^2 \frac{1}{Z_0}(1 - \Gamma^*(z) + \Gamma(z) - |\Gamma(z)|^2)\right] \quad (1) \\
&= \frac{1}{2}\frac{|V_0^+|^2}{Z_0} - \frac{1}{2}\frac{|V_0^+|^2}{Z_0}|\Gamma|^2
\end{aligned}
$$

The equation (1) represents the average power output from the load.

$$P_{load} = P_{IN} - P_{reflection} = P_{IN}(1 - |\Gamma|^2) \tag{2}$$

The power output from the load can be expressed by summing the input power and the reflected power using an equation.

$$\Gamma = (Z_L - Z_0)/(Z_L + Z_0) \tag{3}$$

Equation (3) represents the reflection coefficient formula.

$$P_0 = \frac{1}{2}\frac{|V_0^+|^2}{Z_0} \tag{4}$$

If the impedance satisfies the matching condition, the maximum power can be expressed as Equation (4). Here, we can define the power delivered to the load.

$$P_L = \frac{1}{2}\frac{V_0^2}{Z_0}(1 - \Gamma^2) = P_0(1 - \Gamma^2) = \frac{1}{2}\frac{V_L^2}{Z_L} \tag{5}$$

P_0 represents the maximum input power, V_L denotes the voltage at the load, and Z_L represents the load impedance. The power delivered to the load refers to the difference between the input power and the reflected power.

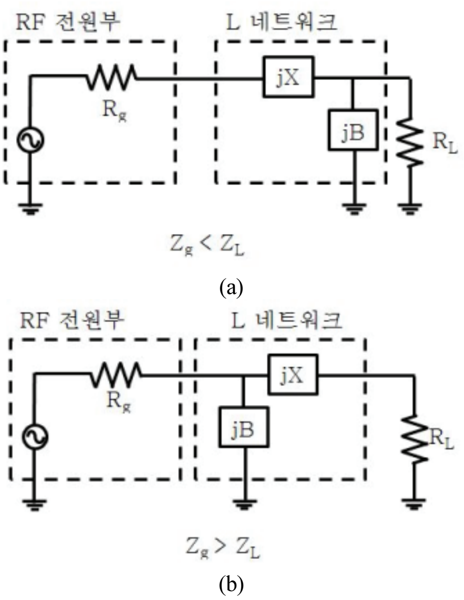

Fig. 3. L-Network calculation using Input Impedance [1].

(a) represents the case where the internal impedance of the power supply is smaller than the load impedance. The internal impedance is defined as follows.

$$Z_0 = jX + \frac{1}{jB + 1/(R_L + jX_L)} \tag{6}$$

Equation (6) can be separated into its real and imaginary parts for analysis.

$$\text{Real part: } B(XR_L - X_L Z_0) = R_L - Z_0 \tag{7}$$

$$\text{Imaginary part: } X(1 - BX_L) = BZ_0 R_L - X_L \tag{8}$$

If we rearrange equations (7) and (8) with respect to X and B, we can obtain the following expressions.

$$B = \frac{X_L + \sqrt{R_L/Z_0}\sqrt{R_L^2 + X_L^2 - Z_0 R_L}}{R_L^2 + X_L^2} \tag{9}$$

$$X = \frac{1}{B} + \frac{X_L Z_0}{R_L} - \frac{Z_0}{BR_L} \tag{10}$$

Equation (b) represents the case where the internal impedance is larger than the load impedance. The input impedance can be expressed as follows.

$$\frac{1}{Z_0} = jB + \frac{1}{R_L + j(X + X_L)} \tag{11}$$

Like equations (7) and (8), the expressions can be divided into real and imaginary parts to confirm the formulas.

$$\text{Real part: } BZ_0(X + X_L) = Z_0 - R_L \tag{12}$$

$$\text{Imaginary part: } X + X_L = BZ_0 R_L \tag{13}$$

When rearranging equations (12) and (13) in terms of X and B, we can obtain the following expressions.

$$B = \pm\frac{\sqrt{(Z_0 - R_L)/R_L}}{Z_0} \tag{14}$$

$$X = \pm\sqrt{R_L(Z_0 - R_L)} - X_L \tag{15}$$

In both cases, if the value of B is positive, it corresponds to a parallel capacitor, and if it is negative, it corresponds to an inductor. Additionally, if the value of X is positive, it corresponds to an inductor, and if it is negative, it corresponds to a capacitor.

In the case of plasma automatic matching systems, the impedance of the load is generally smaller than the internal impedance, so B takes the form of equation (14). If we utilize the previous equation to calculate the load impedance and we also know the input power, we can derive the capacitance values in the matching circuit through mathematical deduction. Correct, since the L-network has a parallel impedance structure, we can deduce the values of the two capacitors.

$$C_1 = \frac{\sqrt{(Z_0 - R_L)/R_L}}{Z_0}\frac{1}{\omega} \tag{16}$$

$$C_2 = \frac{1}{\omega}\frac{1}{\omega L - \sqrt{R_L(Z_0 - R_L)} + X_L} \tag{17}$$

The most simple and widely used matching circuits are L-network and π-network, and this paper utilizes the L-network matching circuit. The structure of the L-network is determined by the internal resistance of the power supply and the load resistance. When the values of the load and power supply impedances are known, it is possible to calculate the appropriate values for the L-network through mathematical formulas. There are two methods that can be used to determine the values of the L-network. One approach is to utilize the Q factor, and the other approach involves calculating the input impedance [4]. The Impedance Matching method is primarily driven by algorithms based on the trends observed in the Phase Magnitude detected by the RF Detector (Phase Sensor) or the trends observed in the V/I (Voltage) detected by the sensor. In this study, the Impedance Matching method based on the intuitive understanding of the V/I (Voltage) trends was chosen.

3. Materials and Methods

To derive the characteristics of Impedance Matching and establish a linear correlation, an experimental setup was created by connecting the RF Generator (13.56 MHz), Power Meter, Phase Sensor, and a Dummy load (50Ω) in that order. This temporary setup allowed for the completion of Impedance Matching, and experiments were conducted under these conditions. The first step involved examining the characteristics of the voltage (V) and current (I) waveforms detected by the Phase Sensor in relation to the input power (W). Furthermore, by incrementing the RF Generator(13.56Mhz, 10~100W) power in 10W increments up to 100W, a linear correlation between the applied power and the voltage (V_1, V_2) and current (I_1, I_2) was observed.

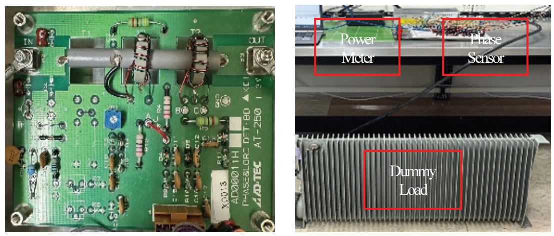

(a) (b)

Fig. 4. Experimental apparatus: (a) A schematic of Phase Senor and (b) A pictorial demonstration of the actual experimental hardware set-up (Impedance Matching).

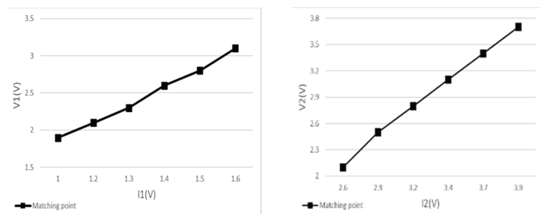

(a) (b)

Fig. 5. Correlation of Voltage: (a) V_1/I_1 and (b) V_2/I_2.

Referring to Fig. 5, it can be observed that with an increase in the applied power from 10W to 100W by the RF Generator(13.56MHz), there is a linear trend in the measured voltages of V_1 and I_1, as well as V_2 and I_2. In case (a) (V_1, I_1), the slope approximates 2, while in case (b) (V_2, I_2), the slope approximates 1.

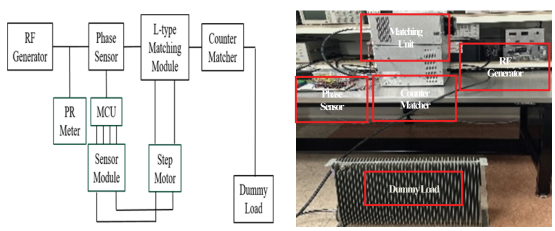

(a) (b)

Fig. 6. Experimental apparatus: (a) A schematic diagram of hardware configuration and (b) A pictorial demonstration of the actual experimental hardware set-up.

Based on these trends, the process of constructing the L-type Impedance Matching Module was carried out before implementing the Impedance Matching algorithm. First, to input the voltage values to the Arduino Mega 2560 acting as the MCU, voltage measurement sensor modules (4 in total) were connected to the Phase Sensor using the voltage division principle to measure the voltage values. Next, to perform Impedance Matching, the capacitance value of the Vacuum Variable Capacitor (VVC) needs to be adjusted by controlling the Step Motor. In the L-Type RF Matcher, two VVCs are used. The capacitor connected in series is called the Tune Capacitor, and the capacitor connected in parallel is called the Load Capacitor. In the L-Type RF Matcher, two VVCs are used. The capacitor connected in series is called the Tune Capacitor, and the capacitor connected in parallel is called the Load Capacitor. The Tune Capacitor is primarily used to compensate for reactive equivalent values, while the Load Capacitor is responsible for matching the equivalent resistance to 50Ω. In the configuration where the Load Capacitor, including the Tune, is facing the load side, both capacitors are adjustable but with different magnitudes. The control algorithm that quickly assesses the harmonization of these adjustable values plays a crucial role in the performance of the RF Matcher. Therefore, in the L-type Matching Module, two Step Motors are used to vary the Capacitance values of the Tune Capacitor and Load Capacitor. First, the environment for driving the Step Motors was set up. Step Motor 1 was configured to operate based on V_1 and I_1 (Load Capacitor) when the number of steps was applied. Similarly, Step Motor 2 was configured to operate based on V_2 and I_2 (Tune Capacitor). Next, an algorithm was designed to allow the Step Motors to rotate and vary the Capacitance values of the VVC based on the desired Step values, which were directly inputted into the serial monitor of the Arduino IDE. Based on the linear trend of Voltage observed in Fig. 5 with respect to the power, the experiment was conducted by determining that Impedance Matching was achieved when the trend of the measured Voltage closely approximated the expected data values. If Step Motor1 and Step Motor2 are driven simultaneously, the reactance value adjusted through the Capacitance of the Tune Capacitor and the equivalent resistance value adjusted through the Capacitance of the Load Capacitor will both change simultaneously. As a result, during the Impedance Matching process, the Voltage values of V and I from the Phase Sensor can vary unpredictably, making it difficult to predict the V/I ratio. Therefore, the process involved first driving Step Motor1 until V_1/I_1 approximated a value close to 2. Once this condition was met, the motor was stopped. Then, Step Motor2 was driven until V_2/I_2 approximated a value close to 1. After achieving this condition, the driving of Step Motor2 was stopped. The Voltage trend observed by the Phase Sensor and the Reflect Power measured by the Power Meter were used to determine if Impedance Matching had been successfully achieved.

4. Results and Discussion

The experimental setup was arranged in the following order: RF Generator, Power meter, Phase Sensor, L-type Matching Unit, Counter Matcher, and Dummy load, as depicted in Fig. 6. The Counter Matcher, serving as a virtual chamber, had a variable Load Capacitor of 100pF and a variable Tune Capacitor of 200pF, allowing for sequential adjustments. This setup simulated the role of a chamber in a real process environment where impedance can arbitrarily change. In addition, the RF power (W) of the RF Generator (13.56MHz) was varied in increments of 20W. The impedance matching conditions were examined at 10W, 30W, and 50W, both before and after impedance matching. The capacitance values of the impedance matching module were measured and compared using an LCR meter.

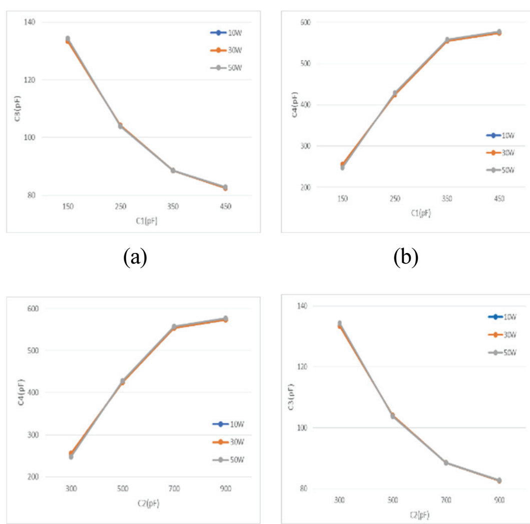

(a) (b)

(c) (d)

Fig. 7. Graph of Capacitance Change: (a) Correlation of C_3/C_1, (b) Correlation of C_4/C_1, (c) Correlation of C_4/C_2 and (d) Correlation of C_3/C_2.

Table 1. Look up Table at 10W

Counter Matcher		Matching Module		Reflect Power	
Load	Tune	Load	Tune	Pr(W)	
C_1 (pF)	C_2 (pF)	C_3 (pF)	C_4 (pF)	Before	After
150	300	133.4	255.9	7.4	0.1
250	500	104.1	424.7	7.9	0.1
350	700	88.5	554.6	7.9	0.2
450	900	82.5	574.2	7.7	0.3

Table 2. Look up Table at 30W

Counter Matcher		Matching Module		Reflect Power	
Load	Tune	Load	Tune	Pr(W)	
C_1 (pF)	C_2 (pF)	C_3 (pF)	C_4 (pF)	Before	After
150	300	133.4	255.9	14.4	0.1
250	500	104.1	424.6	16.0	0.1
350	700	88.5	554.6	17.7	0.2
450	900	82.5	574.2	18.5	0.3

Table 3. Look up Table at 50W

Counter Matcher		Matching Module		Reflect Power	
Load	Tune	Load	Tune	Pr(W)	
C_1 (pF)	C_2 (pF)	C_3 (pF)	C_4 (pF)	Before	After
150	300	134.4	248.1	17.9	0.1
250	500	103.8	429.1	19.9	0.1
350	700	88.5	558.3	19.9	0.2
450	900	82.8	577.1	19.9	0.3

Fig. 7 illustrates the correlation between the capacitance values of the Counter Matcher acting as a virtual chamber (Load: C_1, Tune: C_2) and the capacitance values of the L-type Matching Unit (Load: C_3, Tune: C_4) in relation to the applied power (10W, 30W, 50W) from the RF Generator (13.56MHz). It can be observed from (a) that the capacitance (C_1) of the Counter Matcher's Load Capacitor and the capacitance (C_3) of the Matching Module's Load Capacitor exhibit an inverse relationship, where an increase in C_1 results in a decrease in C_3. (b) demonstrates that the capacitance(C_1) of the Counter Matcher's Load Capacitor and the capacitance(C_4) of the Matching Module's Tune Capacitor exhibit a similar increasing trend as C_1 increases. (c) demonstrates that the capacitance(C_2) of the Counter Matcher's Tune Capacitor and the capacitance(C_4) of the Matching Module's Tune Capacitor exhibit a similar increasing trend as C_2 increases. Finally, (d) shows that the capacitance(C_2) of the Counter Matcher's Tune Capacitor and the capacitance(C_3) of the Matching Module's Load Capacitor exhibit a similar decreasing trend as C_2 increases. At 10W and 30W, the capacitance values of the Tune Capacitor, which adjusts the equivalent resistance value of the L-type Matching Module, were found to be the same. However, at 50W, there were discrepancies [(C_1: 150pF, C_2: 300pF): 7.8pF / (C_1: 250pF, C_2: 500pF): -4.5pF / (C_1: 350pF, C_2: 700pF): -3.7pF / (C_1: 450pF, C_2: 900pF): -2.9pF] compared to the capacitance values at 10W and 30W. This indicates that Impedance Matching was achieved at 50W. The capacitance values for compensating the reactance equivalent, Load Capacitor, are the same at (C_1: 150pF, C_2: 300pF) and (C_1: 350pF, C_2: 700pF). However, for the other conditions, there is an error [(C_1: 250pF, C_2: 500pF): 0.3pF / (C_1: 450pF, C_2: 900pF): -0.3pF] observed. In the Impedance Matching environment, the Reflect Power shows the same value [(C_1: 150pF, C_2: 300pF) / (C_1: 250pF, C_2: 500pF): 0.1W / (C_1: 350pF, C_2: 700pF): 0.2W / (C_1: 450pF, C_2: 900pF): 0.3W] for the applied power levels (10W, 30W, 50W). Additionally, it can be observed that as the values of Counter Matcher's Load Capacitor and Tune Capacitor increase, the Reflect Power also slightly increases. Counter Matcher's VVC and Matching Module's VVC having different capacitance values due to the Counter Matcher's VVC capacitance variation can be attributed to several factors. Firstly, before conducting the impedance matching, a specific starting position for C_3 and C_4 within the matching device (L-type Matching Unit) is set, which corresponds to the hardware limit where the VVCs (C_3 and C_4) no longer rotate. During the process of varying the Counter Matcher's Load and Tune Capacitor capacitance by directly applying step counts using the Arduino IDE, the Counter Matcher's capacitance reaches the hard-ware limit. To achieve precise impedance matching, it is necessary to apply precise microsteps to the Step Motors of the Matching Module. However, limitations of the MCU (Arduino Mega 2560) used in the experiment and the restricted external power specifications of the Arduino Mega 2560 prevent the Step Motor from being controlled with higher precision torque. Furthermore, after completing the matching, when directly measuring the capacitance with an LCR Meter by detaching the VVCs, the axis of the VVCs was not completely fixed, leading to slight variations in the capacitance readings. Considering these factors, it can be concluded that the combination of the MCU limitations, the restricted torque control, and the unsecured axis of the VVCs contributed to the differences in capacitance values of the VVCs. This can be resolved by selecting a higher capacity Step Motor Driver and Step Motor that are compatible with the external power requirements of the Matching Module configuration. Theoretically, when Impedance Matching is achieved, the Reflect Power should converge to zero. However, a slight Reflect Power was observed compared to the applied power, which was determined to be influenced by the lengths of the coaxial lines connecting the RF Generator(13.56MHz), Phase Sensor, L-type Matching Module, Counter Matcher, and Dummy Load. In order to conduct the experiment, RF signals were applied using an RF Generator(13.56MHz). The high frequency signal travels through the coaxial line at a specific frequency, and depending on the frequency and length, it exhibits a consistent waveform pattern. If the length of the coaxial line does not correspond to the wavelength of the incident waves, it can result in impedance mismatching, leading to signal loss and reflections. This can have an impact on signal quality and transmission distance. Therefore, the lack of precise calculation of the coaxial line length and the limitations in setting up the experimental equipment resulted in the use of self-made coaxial lines that varied in length based on the distance of the experimental setup. This contributed to the presence of slight reflect power in the measurements. Therefore, in order to achieve accurate impedance matching, it is necessary to construct the length of the coaxial line as an integer multiple of the wavelength of the incident signal. By minimizing the reflection and loss of RF signals through the coaxial line, it is judged that the slight measured reflect power can be sufficiently resolved and converge to zero.

5. Conclusions

Through this project, we were able to understand and comprehend the structure and principles of the Phase Sensor, which detects RF signals, as well as the configuration of the L-type RF Matcher. Based on the trends of the voltage detected at the V Probe and the EMF voltage detected at the I Probe, we designed a Step Motor Control algorithm. Through this, we were able to perform Impedance Matching using VVC control of the L-type Matching Module and understand the trends of the Capacitance when Impedance Matching is achieved. Correctly detecting the period and waveform of the RF signal using the Phase Sensor, utilizing a Coaxial line with a length that is an integer multiple of the half-wavelength of the detected signal, and achieving finer Step Motor Control for VVC capacitance variation can indeed lead to the expectation of achieving theoretical Impedance Matching.

Acknowledgement

This research is the result of an undergraduate industry academia project supported by the Semiconductor Major Track Program. We would like to express our gratitude to Professor Dae Sik Junn from the Department of Semiconductor Engineering for his support in setting up the RF equipment and providing valuable advice throughout the research process.

References

1. K. H. Jang, "A Study on the Implementation of Auto Impedance Matching circuit for a Plasma Application at 13.56MHz", Master's Thesis, Kwangwoon University, 2014.
2. K. H. Jang, S. Y. Park, J. J. Choi, and D.-H. Lee, "Error Rate Enhancement Algorithm for 13.56 MHz Impedance Automatic Matching System", "The journal of Korean Institute of Electromagnetic Engineering and Science, Vol. 29, No. 7, pp. 484-490, 2018.
3. H. Y. Jang, "Semiconductor/Display Manufacturing Process Plasma Foundation and Application", The Korean Information Display Society, Vol. 12, No. 5, pp. 2-15, 2011.
4. H. G. Kim, J. W. Yang, S. H. Kang, D. H. Choi, and S. J. Hong, "RF Impedance Matching Algorithm Using Phase Detector", The Korean Society of Semiconductor & Display Technology, Vol. 21, No. 2, 2022.

5. J. H. Lee, H. K. Park, J. S. Lee, and S. J. Hong, "Understanding of RF Impedance Matching System Using VI-Probe", The Korean Society of Semiconductor & Display Technology, Vol. 19, No. 3, pp. 43-48, 2020.
6. W. S. Kang, "A Study on Dual Impedance Matching Technique for Improving Efficiency of RF System with Variable Impedance", Ph.D. Thesis, Konkuk University, 2018.
7. D. G. Choi and W. J. Jang, "Plasma Generator & Auto Matching Network", Journal of the Korean Institute of Illuminating and Electrical Installation Engineers 1995 Autumn Conference, pp. 60-63, 1995.
8. D. W. Shin, "High-speed Impedance Matching with Gradient Descent for an Advanced Radio Frequency Plasma System", Master's Thesis, Myongji University, 2023.

접수일: 2023년 6월 2일, 심사일: 2023년 6월 16일,
게재확정일: 2023년 6월 21일